



AEROSOL NUCLEATION AND GROWTH DURING LAMINAR TUBE FLOW: MAXIMUM SATURATIONS AND NUCLEATION RATES

J. C. Barrett*[†] and T. J. Baldwin[†]

*Department of Nuclear Science and Technology, HMS SULTAN, Military Road, Gosport PO12 3BY, U.K.

[†]Department of Chemistry, University of Surrey, Guildford, Surrey GU2 5XH, U.K.

(First received 25 May 1999; and in final form 23 August 1999)

Abstract—An approximate method of estimating the maximum saturation, the nucleation rate, and the total number nucleated per second during the laminar flow of a hot vapour–gas mixture along a tube with cold walls is described. The basis of the approach is that the temperature and vapour concentration differences between the wall and a point in the tube are approximately proportional to $R(r)Z(z)$ and $R(r)F(Z(z))$, respectively, where r and z are dimensionless radial and axial coordinates and R , Z , and F are known functions. Key parameters determining the location and magnitude of the maximum saturation are the Lewis number, Le , and a parameter, B , which determines the temperature variation of the equilibrium vapour concentration (B is roughly the latent heat of vaporisation per vapour molecule divided by Boltzmann's constant). For vapour–gas mixtures with $Le > 1$, the maximum saturation occurs at the tube axis but for those with $Le < 1$ it occurs near the tube wall. The magnitude of the maximum saturation achieved increases rapidly with B . The approach assumes that condensation on previously nucleated particles is negligible, and a condition on the maximum nucleation rate for this to be so is derived. Predictions are compared with numerical calculations for DBP vapour and for water vapour and very good agreement is found. The approach is used in conjunction with Hale's scaled nucleation theory to determine the tube wall–inlet temperature difference needed to achieve various nucleation rates for any specified vapour–gas mixture. This approach can be applied to many other two-dimensional systems where simultaneous heat and mass transfer occur provided that the temperature and vapour concentration can be expressed in the forms given above. Crown Copyright © 2000/MOD. Published by Elsevier Science Ltd. All rights reserved

NOMENCLATURE

- A constant in continuum growth rate expression, $\dot{R} = A/R_d$, $m^2 s^{-1}$
 a_i constants in equation (5) ($a_1 \approx 1.4764$).
 B constant in equilibrium vapour concentration equation, $c_c(T) = c_\infty \exp(-B/T)$, K
 D diffusivity of vapour in gas, $m^2 s^{-1}$
 c vapour concentration, ρ_v/ρ
 c_w vapour concentration on tube wall, $c_w = c_c(T_w)$
 Δc vapour concentration difference between inlet and tube wall
 c_∞ constant in equilibrium vapour concentration expression, $c_c(T) = c_\infty \exp(-B/T)$
 $c_c(T)$ equilibrium vapour concentration at temperature T
 c_p specific heat capacity of vapour–gas mixture at constant pressure, $J kg^{-1} K^{-1}$
 c_{pg} specific heat capacity of gas at constant pressure, $J kg^{-1} K^{-1}$
 c_{pv} specific heat capacity of vapour at constant pressure, $J kg^{-1} K^{-1}$
 Cn condensation number, $Cn = k/\{LD\rho c_c(T)\}$
 $f(T)$ temperature dependent part of exponential in equation (3)
 J nucleation rate, $m^{-3} s^{-1}$
 $J_p(r)$ peak nucleation rate at radial position r , $m^{-3} s^{-1}$
 k thermal conductivity of vapour–gas mixture, $W m^{-1} K^{-1}$
 k_B Boltzmann's constant ($\approx 1.38 \times 10^{-23}$), $J K^{-1}$
 K pre-exponential factor in nucleation rate expression, equation (3), $m^{-3} s^{-1}$
 L latent heat of condensation of vapour, $J kg^{-1}$
 Le Lewis number $k/\{c_p\rho D\}$
 m_1 mass of one vapour molecule, kg
 \dot{m}_v condensation rate on nucleated aerosol, $kg m^{-3} s^{-1}$
 M total mass condensed on nucleated aerosol at position z_p , kg
 $n(R_d, t)$ aerosol size distribution at time t , m^{-4}

[†] Author to whom correspondence should be addressed.

$N(r)$	total number nucleated per second at radial position r , $\text{m}^{-2} \text{s}^{-1}$
N_{tot}	total number of droplets nucleated in tube per second, s^{-1}
N_{out}	number concentration at tube outlet, m^{-3}
$p_{\text{ve}}(T)$	equilibrium vapour pressure at temperature T , N m^{-2}
r	dimensionless radial coordinate, r'/r_0
r_0	tube radius, m
r_c	dimensionless radius at which S_{max} from equation (9) equals S_{max} from equation (11)
r'	radial distance from tube axis, m
$R(r)$	approximate radial variation of θ , i.e. $\theta(r, z) \approx R(r)Z(z)$
R_d	droplet radius, m
\dot{R}	droplet growth rate, m s^{-1}
S	vapour saturation
T	temperature, K
T_c	critical temperature of vapour, K
T_p	temperature at location of peak nucleation rate, K
T_w	tube wall temperature, K
ΔT	temperature difference between inlet and wall, K
δT	temperature difference given by equation (8), K
δT_1	temperature difference given by equation (10), K
$v(r)$	axial flow velocity at dimensionless radial position r , m s^{-1}
v_1	molecular volume, $v_1 = m_1/\rho_1$, m^3
V_M	axial flow velocity on tube axis, m s^{-1}
z	dimensionless axial distance, $z = z'/(r_0^2 V_M)$
z_0	dimensionless axial position of maximum saturation
z_p	dimensionless axial position of maximum nucleation rate
z'	axial distance from tube inlet, m
$Z(z)$	approximate axial variation of θ , i.e. $\theta(r, z) \approx R(r)Z(z)$

Greek letters

α	thermal diffusivity, $\alpha = k/(c_p \rho)$, $\text{m}^2 \text{s}^{-1}$
β_i	parameters in equation (5); $\beta_1 \approx 2.704$, $\beta_2 \approx 6.679$
γ	surface tension, J m^{-2}
ε	correction term to account for difference between position of max. S and of max. J
θ	dimensionless function in equations (4a) and (4b)
λ	minus the coefficient of r^2 in $\chi_1(r)$, $\lambda \approx 1.8284$
ρ	total (vapour + gas) density, kg m^{-3}
ρ_l	liquid density, kg m^{-3}
ρ_v	vapour density, kg m^{-3}
$\rho_{\text{ve}}(T)$	equilibrium vapour density at temperature T , kg m^{-3}
σ_z	parameter in equation (16)
σ_r	parameter describing radial variation of $J_p(r)$, i.e. $J_p(r) = J_p(0) \exp(-r^2/2\sigma_r^2)$
$\chi_i(r)$	functions in equation (5)
Ω	dimensionless parameter in equation (29) ($\Omega = 2.35$ in calculations)

1. INTRODUCTION

Homogeneous nucleation is an important process in many environmental and industrial systems. The laminar flow diffusion chamber is a device used in the laboratory to examine nucleation and condensation processes and there have been several experimental and modelling studies of nucleation in this device published in recent years (see Nguyen *et al.*, 1987; Vohra and Heist, 1996; Hämeri *et al.*, 1996; Wilck *et al.*, 1998, and references therein). However, the modelling work has usually concentrated on a specific device and vapour, with attributes such as tube dimensions, temperatures, and flow rates fixed (or varying over limited range).

Our interests are somewhat different, being mainly concerned with industrial processes where a wide range of thermal conditions may occur and a variety of vapours (often with poorly known thermodynamic properties) are of interest. We want to explore the range of conditions for nucleation to occur and, if it does, to estimate its location as well as the total number of particles produced. Our approach, described in Section 2, is to develop simplified analytical approximations that allow these features, and their dependence on key parameters, to be identified. In this paper we concentrate on the limit where vapour depletion by condensation on particles is negligible, and we provide a condition for this approximation to be valid. In Section 3, we compare results from our approximate treatment with more accurate numerical calculations for dibutyl phtalate (DBP) and for water. We then

demonstrate how our approach can provide insights into experimental results and predictions for the behaviour of other vapours. We summarise our findings in the final section.

2. FORMALISM

The equations describing the temperature T and vapour concentration c during axisymmetric laminar flow of a vapour-gas mixture along a tube of radius r_0 are (Barrett and Fissan, 1989):

$$c_p \rho v \frac{\partial T}{\partial z'} + \frac{1}{r'} \frac{\partial}{\partial r'} \left(-kr' \frac{\partial T}{\partial r'} \right) - (c_{pv} - c_{pg}) D \rho \frac{\partial c}{\partial r'} \frac{\partial T}{\partial r'} = L \dot{m}_v, \tag{1}$$

$$\rho v \frac{\partial c}{\partial z'} + \frac{1}{r'} \frac{\partial}{\partial r'} \left(-D \rho r' \frac{\partial c}{\partial r'} \right) = -(1 - c) \dot{m}_v, \tag{2}$$

where \dot{m}_v is the condensation rate per unit volume onto any aerosol present. Our key assumption in this paper is that the terms involving \dot{m}_v in equations (1) and (2) can be ignored. Since condensation raises the temperature of the mixture (due to latent heat release) and reduces the vapour concentration, ignoring condensation yields the highest possible value for the vapour saturation S and therefore for the homogeneous nucleation rate $J(S, T)$ which is assumed to have the form

$$J(S, T) = K \exp\left(-\frac{f(T)}{(\ln S)^2} \right). \tag{3}$$

Equation (3) is the same as the classical expression, modified by a factor $1/S$ (see Oxtoby, 1992), if we take $K = \sqrt{2\gamma}/(\pi m_1) v_1 (c\rho/m_1)^2/S$ and $f(T) = (16\pi/3)v_1^2 \gamma^3/(k_B T)^3$, with the molecular volume $v_1 = m_1/\rho_1$. For small c , the saturation is given in terms of the vapour concentration and temperature by, $S \approx c/c_e(T)$.

In all the following, we ignore the temperature variation of transport properties (k, D , and viscosity μ) and assume the total density of the vapour-gas mixture flowing along the tube is constant. Then we can use the parabolic form for the velocity profile, $v(r) = V_M(1 - (r'/r_0)^2)$. Provided the boundary conditions are suitable (e.g. constant vapour concentration at the wall), equation (2) can be solved analytically by separation of variables. This is also true of equation (1), if we ignore the final term on the left-hand side, which represents heat transfer by the diffusing vapour. In many circumstances, the vapour concentration is so small that this term can be neglected; however, it was found to be significant in calculations for water vapour at moderate temperatures (Barrett and Clement, 1986). Ignoring this term, the analytical solutions can be conveniently written in terms of the dimensionless variables $r = r'/r_0$ and $z = z'\alpha/(r_0^2 V_M)$,

$$T(r, z) = T_w + \Delta T \theta(r, z), \tag{4a}$$

$$c(r, z) = c_w + \Delta c \theta(r, z/Le), \tag{4b}$$

where T_w is the (constant) wall temperature and ΔT is the difference between the inlet and wall temperatures (and similarly for c_w and Δc) and $Le = \alpha/D$ is the Lewis number (the ratio of thermal diffusivity to vapour-gas diffusion coefficient, D). The $\theta(r, z)$ is given by

$$\theta(r, z) = \sum_{i=1}^{\infty} a_i \chi_i(r) \exp(-\beta_i^2 z), \tag{5}$$

where the a_i and β_i are known constants and the χ_i are functions that can be expressed as infinite series in powers of r^2 . Equation (5) is the well-known Nusselt-Graetz solution (Nusselt, 1910, but see also Ingham, 1975). We now assume that c is small, so $S \approx c/c_e(T)$,

and that $c_e(T)$ has the form $c_e(T) = c_\infty \exp(-B/T)$ where c_∞ and B are constants. Then,

$$S(r, z) = \frac{c}{c_e(T)} = \frac{[c_w + \Delta c \theta(r, z/Le)]}{c_\infty} \exp\left(\frac{B}{T_w + \Delta T \theta(r, z)}\right). \tag{6}$$

As discussed previously (Baldwin and Barrett, 1998; see also Larrode *et al.*, 1998) we can use equation (6) to find the approximate value of the maximum saturation achieved along any streamline (i.e. at fixed r). For $Le = 1$, only $\theta(r, z)$ appears in equation (6) and we can set $dS/d\theta = 0$ to find the position of the maximum of S . This gives a quadratic for θ , the relevant solution of which is given to a very good approximation by $\delta T \equiv \Delta T \cdot \theta_{\max} = (T_w^2 - B\Delta T c_w/\Delta c)/(B - 2T_w) \approx T_w^2/(B - 2T_w)$. The final form follows if $c_w \ll \Delta c$, which will often be the case. The physical interpretation of δT is that it is the temperature difference between the wall and the position of the maximum saturation.

To obtain simple results in the case $Le \neq 1$, we assume that $\theta(r, z)$ is given by the first term in the series, equation (5). Since $\beta_1 \approx 2.704$ and $\beta_2 \approx 6.679$, this should be a reasonable approximation provided z is greater than about 0.05. Then, writing $Z(z) = \exp(-\beta_1^2 z)$ and $R(r) = a_1 \chi_1(r)$, we have $\theta(r, z) = RZ$ and $\theta(r, z/Le) = RZ^{1/Le}$. Setting $\partial S/\partial Z = 0$ at $z = z_0$ gives the following equation for $Z(z_0)$:

$$\left(\frac{\delta c}{c_w + \delta c}\right) \frac{1}{Z(z_0)Le} - \frac{B\Delta TR(r)}{[T_w + \Delta TR(r)Z(z_0)]^2} = 0, \tag{7}$$

where $\delta c = \Delta c \theta(r, z_0/Le)$ is the concentration difference between the position of maximum saturation and the wall. Assuming $\delta c \gg c_w$ (so the first term, in large brackets, can be replaced by unity), equation (7) has a solution very similar to that found before:

$$\delta T \equiv \Delta T \cdot R(r)Z(z_0) \approx \frac{T_w^2}{BLE - 2T_w}. \tag{8}$$

According to equation (8), as we vary the radial coordinate, r , the axial position of the maximum saturation varies, but the temperature at the maximum saturation, $T_w + \delta T$, is independent of radial position. Using the known values of a_1 (≈ 1.4764) and $\chi_1(r)$, equation (8) allows us to determine $Z(z_0)$ and hence the axial location of the maximum saturation, $z_0 = -\ln(Z)/\beta_1^2$. From equation (6), we obtain the maximum saturation at a given radial position in terms of Z or R ;

$$\begin{aligned} S_{\max} &= \frac{\delta T}{\Delta T} \exp\left(\frac{B}{T_w + \delta T} - \frac{B}{T_w + \Delta T}\right) Z^{(Le^{-1}-1)} \\ &= \left(\frac{\delta T}{\Delta T}\right)^{Le^{-1}} \exp\left(\frac{B}{T_w + \delta T} - \frac{B}{T_w + \Delta T}\right) R^{(1-Le^{-1})}, \end{aligned} \tag{9}$$

where we have assumed that the inlet is saturated so $\Delta c \approx c_\infty \exp(-B/[T_w + \Delta T])$. The second form follows by using equation (8). From equations (8) and (9), we predict that S_{\max} will be large if B is large, and that it increases with increasing Le . Also, since $R(r) = a_1 \chi_1(r)$ decreases as r increases, equation (9) shows that if $Le > 1$ then S_{\max} is greatest at the tube axis, but if $Le < 1$, S_{\max} increases as r increases towards 1. However, near the wall, the above treatment breaks down since it is no longer sufficient to consider only the first term in the series expansion, equation (5). Instead, we use the boundary layer solution for $\theta(r, z)$, derived by L ev eque (1928), which is valid for small z . Near the wall (i.e. if $(1-r)/z^{1/3} \ll 1$ in addition to $z \ll 1$), this solution is approximately $\theta(r, z) \approx \{3^{1/3}/\Gamma(1/3)\} (1-r)/z^{1/3}$, where $\Gamma(x)$ is the gamma function. Then, putting $R(r) = 1-r$ and $Z(z) = 3^{1/3}/\{\Gamma(1/3)z^{1/3}\}$, we have $\theta(r, z) = R(r)Z(z)$ and $\theta(r, z/Le) = R(r)Z(z)Le^{1/3}$. Setting $\partial S/\partial Z = 0$ gives an equation with (approximate) solution for δT identical to the $Le = 1$

case, except that Δc is replaced by $\Delta c \text{Le}^{1/3}$,

$$\delta T_1 \approx \frac{T_w^2 - Bc_w \Delta T / (\Delta c \text{Le}^{1/3})}{B - 2T_w} \quad (1-r) \ll 1. \quad (10)$$

The maximum saturation in this case is

$$S_{\max} = \left[1 + \frac{c_w \Delta T}{\delta T_1 \Delta c \text{Le}^{1/3}} \right] \text{Le}^{1/3} \frac{\delta T_1}{\Delta T} \exp\left(\frac{B}{T_w + \delta T_1} - \frac{B}{T_w + \Delta T} \right) \quad (1-r) \ll 1. \quad (11)$$

Equations (10) and (11) simplify if we set $c_w = 0$, as done in the derivation of equations (8) and (9). However, we find that the terms involving c_w are not negligible for water at temperatures of interest (see next section).

The nucleation rate depends on temperature and saturation, both of which are varying in the tube, consequently the maximum nucleation rate will not in general coincide with the maximum saturation. From equation (3), ignoring the much weaker dependence of the prefactor K with T and S , the condition $\partial(\ln J)/\partial z = 0$ can be written as

$$\frac{-f(T)}{(\ln S)^2} \left[\frac{f'(T)}{f(T)} \frac{\partial T}{\partial z} - \frac{2}{\ln S} \frac{\partial(\ln S)}{\partial z} \right] = 0. \quad (12)$$

To estimate the value of $Z(z_p)$ at which this equation is satisfied, we write

$$Z(z_p) = Z(z_0)(1 + \varepsilon), \quad (13)$$

where ε is assumed to be small. Expanding equation (12) to first order in ε and making some other reasonable approximations, we can obtain an expression for ε . Details are given in the appendix. Near the tube axis, the result is

$$\varepsilon = -\frac{1}{2} \text{Le} \ln(S_{\max}) \delta T \frac{f'(T_w + \delta T)}{f(T_w + \delta T)}. \quad (14)$$

where S_{\max} is given by equation (9) and δT by equation (8). The peak nucleation rate, J_p is calculated from equation (3) using a temperature $T_p = T_w + \delta T(1 + \varepsilon)$ and saturation $S_p = S_{\max}$. Near the tube walls,

$$\varepsilon = -\frac{1}{2} \ln(S_{\max}) \delta T_1 \frac{f'(T_w + \delta T_1)}{f(T_w + \delta T_1)}, \quad (15)$$

where S_{\max} is given by equation (11), and δT_1 by equation (10).

To estimate the width of the nucleation peak, and therefore the number of particles nucleated, we assume that, for fixed r , $J(r, z)$ can be represented by a Gaussian around J_p , i.e.

$$J(r, z) = J_p(r) \exp\left(-\frac{(z - z_p)^2}{2\sigma_z^2} \right). \quad (16)$$

Expressions for σ_z are found by equating the second derivative with respect to z of equations (3) and (16) at the nucleation (actually saturation) peak. Details are given in the appendix. The results are:

Near the tube axis:

$$\sigma_z \approx \left[\frac{(\ln S_{\max})^3 \text{Le}}{2f(T)} \right]^{1/2} \frac{1}{\beta_1^2}. \quad (17)$$

Near the tube wall:

$$\sigma_z \approx 3z_0 \left[\frac{(\ln S_{\max})^3}{2f(T)} \right]^{1/2} = 9 \left(\frac{(1-r)\Delta T}{\Gamma(1/3)\delta T_1} \right)^3 \left[\frac{(\ln S_{\max})^3}{2f(T)} \right]^{1/2}, \tag{18}$$

where the final form follows by substituting for z_0 using the relation $\delta T_1 \equiv \Delta T.R(r)Z(z_0)$, with the appropriate forms of R and Z near the wall.

The total number of particles nucleated per second at a given tube radius can be found from

$$N(r) = \int_0^\infty J(r, z) dz' = \frac{r_0^2 V_M}{\alpha} \int_0^\infty J(r, z) dz \approx \frac{r_0^2 V_M}{\alpha} J_p(r) \sqrt{2\pi} \sigma_z, \tag{19}$$

where we have assumed that the tube length is sufficient to ensure that all nucleation takes place before the end. To find the total number of particles flowing along the tube (integrated over tube radius), we need to consider the radial variation of J_p . The cases $Le > 1$ and $Le < 1$ will be treated separately.

For $Le > 1$, we can represent $J_p(r)$ as a Gaussian about $r = 0$, i.e. $J_p(r) = J_p(0) \exp(-r^2/2\sigma_r^2)$, where σ_r is found by calculating the second derivative of $\ln J$ from equation (3). The result is (see the appendix)

$$\sigma_r \approx \left[\frac{(\ln S)^3}{2f(T)} \right]^{1/2} \frac{1}{\sqrt{2\lambda(1 - Le^{-1})}}, \tag{20}$$

where $\lambda \approx 1.8284$ is minus the coefficient of the r^2 term in $\chi_1(r)$. Using equation (19) we then have for the total number of particles flowing down the tube per second,

$$N_{\text{tot}} = 2\pi \int_0^{r_0} r' N(r) dr' \approx \frac{r_0^4 V_M}{\alpha} J_p(0) (2\pi)^{3/2} \sigma_z \sigma_r^2. \tag{21}$$

For $Le < 1$, nucleation occurs near the wall, and we assume that the maximum rate is independent of r for r greater than some value r_c . We estimate r_c by equating the value of S_{\max} for equation (9), valid near the axis, to that from equation (11), valid near the wall. Using $Z = \delta T / (\Delta T a_1 \chi_1(r_c))$ (from equation (8)), we find,

$$\begin{aligned} \chi_1(r_c) &= \frac{\delta T}{a_1 \Delta T} \left(\left[1 + \frac{c_w \Delta T}{\delta T_1 \Delta c Le^{1/3}} \right] Le^{1/3} \right. \\ &\quad \left. \times \frac{\delta T_1}{\delta T} \exp \left[\frac{B}{T_w + \delta T_1} - \frac{B}{T_w + \delta T} \right] \right)^{Le/(Le-1)}. \end{aligned} \tag{22}$$

As a first approximation, we set $\chi_1(r_c) = 1 - r_c$ near the wall.

To evaluate N_{tot} , we assume that $J_p(r)$ is constant (with its value calculated at $T = T_w + \delta T_1(1 + \varepsilon)$ and $S = S_{\max}$ given by equation (11)) for $r_c < r < 1$, and zero for $r < r_c$. Then,

$$\begin{aligned} N_{\text{tot}} &= 2\pi r_0^2 \int_0^1 r N(r) dr \approx (2\pi)^{3/2} \frac{r_0^4 V_M}{\alpha} J_p(1) \int_{r_c}^1 \sigma_z r dr \\ &= 9(2\pi)^{3/2} \frac{r_0^4 V_M}{\alpha} J_p(1) \left(\frac{\Delta T}{\Gamma(1/3)\delta T_1} \right)^3 \left(\frac{\ln S_{\max}}{2f(T)} \right)^{1/2} \\ &\quad \times \left\{ \frac{1}{4} (1 - r_c)^4 - \frac{1}{5} (1 - r_c)^5 \right\}, \end{aligned} \tag{23}$$

where we have used equation (18) for σ_z and performed the integration with respect to r . By $J_p(1)$ we mean the peak nucleation rate near the wall, i.e. calculated at $T_p = T_w + \delta T_1(1 + \varepsilon)$ and $S = S_{\max}$ with ε given by equation (15), δT_1 by equation (10) and S_{\max} by equation (11).

It is interesting to note that, for both $Le < 1$ and $Le > 1$, the maximum saturation and nucleation rate in the tube are independent of tube radius, r_0 , and flow velocity V_M . Furthermore, since N_{tot} is proportional to $V_M r_0^4$, the number concentration at the outlet (equal to N_{tot} divided by the volumetric flow rate, $\pi V_M r_0^2/2$) is independent of flow rate and proportional to the tube cross-sectional area.

The key assumption in our approach is that vapour condensation on previously nucleated particles is not sufficient to affect the nucleation of new particles. We can obtain an approximate condition for this assumption to be valid by adapting a method used previously to estimate the number of particles formed in a nucleation burst (Barrett and Clement, 1991). Consider a streamline parallel to the tube axis at (dimensionless) radial position r . The total mass per unit volume condensed on particles at dimensional position z'_p (corresponding to the position of maximum nucleation in the absence of condensation) is

$$M = \int_0^{z'_p} \dot{m}_v \frac{dz'}{v(r)} = \frac{4\pi\sigma_1 r_0^2}{\alpha(1-r^2)} \int_0^{z'_p} dz \int_0^\infty dR_d R_d^2 \dot{R} n(R_d, t), \tag{24}$$

where R_d is the droplet radius and $n(R_d, t)$ is the size distribution of the nucleated aerosol. We can estimate M by using the size distribution ignoring the effect of vapour depletion in this equation. If $R_d(z, \hat{z})$ represents the radius at (dimensionless) position z of a droplet nucleated at (dimensionless) position \hat{z} , then the integral over R_d can be transformed into an integral over \hat{z} ,

$$M = \frac{4\pi\rho_1 r_0^4}{\alpha^2(1-r^2)^2} \int_0^{z'_p} dz \int_0^z d\hat{z} R_d(z, \hat{z})^2 \dot{R} J(r, \hat{z}). \tag{25}$$

We now use the Gaussian expression, equation (16), for $J(r, z)$ and assume continuum growth with $\dot{R} = A/R_d$, so $R_d(z, \hat{z}) = \sqrt{2Ar_0^2(z - \hat{z})/(\alpha[1 - r^2])}$. Substituting these expressions into equation (25) and performing the integrals (most easily by first reversing the order of integration), we obtain

$$M = \frac{2^{7/4}\pi\Gamma(1/4)}{3} \frac{\rho_1 r_0^5 A^{3/2} \sigma_z^{5/2}}{\alpha^{5/2}(1-r^2)^{5/2}} J_p(r), \tag{26}$$

where we have assumed that the nucleation peak occurs well within the tube, i.e. $z_p \gg \sigma_z$, so that we can replace the lower limit of the integral over \hat{z} by $-\infty$. We have also used the recurrence relation for the gamma function, $\Gamma(x + 1) = x\Gamma(x)$.

This condensation reduces the vapour saturation both by removing vapour and by raising the temperature (due to the release of latent heat). The change in saturation caused is approximately (Barrett and Clement, 1991) $-M(1 + S_{\max} Le/Cn)/[\rho_c(T_p)]$, where Cn is the condensation number (Clement, 1985) giving the ratio of conductive heat transfer to latent heat carried by the mass current. The change in saturation needed to reduce the nucleation rate by a factor e from its value at the peak is approximately $-S_{\max} [\ln S_{\max}]^3/2f(T_p)$ and we require the change in S caused by the condensation M to be less than this for our approach to be valid. This can be rearranged into a condition on the peak nucleation rate $J_p(r)$ for vapour condensation to be negligible,

$$J_p(r) \ll \frac{3}{2^{11/4}\pi\Gamma(1/4)} \frac{(\ln S_{\max})^3}{f(T_p)} \frac{\alpha^{5/2}}{A^{3/2}} \left(\frac{\rho_v}{\rho_l}\right) \left[\frac{(1-r^2)^{5/2}}{1 + S_{\max} Le/Cn} \right] \frac{1}{\sigma_z^{5/2} r_0^5}. \tag{27}$$

Rather than consider this general condition further, we restrict our attention to substances with $Le > 1$ and $Cn \gg 1$ (e.g. large organic molecules with low vapour densities and latent heats). For the growth rate constant we use $A = D\rho c_e(T_p)(S_{\max} - 1)/\rho_1$. We also assume that $S_{\max} \gg 1$, but $S_{\max} Le/Cn \ll 1$. Then, on the tube axis ($r = 0$), equation (27) becomes

$$J_p(0) \ll \frac{3\beta_1^5}{2^{3/2}\pi\Gamma(1/4)} \left[\frac{Le f(T_p)}{(\ln S_{\max})^3} \right]^{1/4} \alpha \left(\frac{\rho_1}{S_{\max}\rho_{ve}(T_p)} \right)^{1/2} \frac{1}{r_0^5}. \quad (28)$$

The right-hand side of this inequality decreases with increasing temperature, but the main dependence is the r_0^{-5} variation with tube radius.

3. RESULTS

To assess the accuracy of the approximate approach described in the previous section, we need accurate solutions of equations (1) and (2). Although, for $\dot{m}_v = 0$, an analytical solution is available (i.e. equation (5)) provided we ignore the final term on the right in equation (1), a large number of terms in the infinite series are needed near the tube entrance. We therefore used a numerical solution of these equations, obtained by the method of orthogonal collocation. This method is described in detail by Finlayson (1972) and its application to laminar tube flow is discussed by Barrett and Fissan (1989). The accuracy of the method increases with the number of quadrature points used; Finlayson tabulates values for up to 6 quadrature points, the higher order quadrature schemes were obtained from the recurrence relation between polynomials orthogonal to weighting function $r(1 - r^2)$, using the subroutine GAUCOF (Press *et al.*, 1992). We used 8 or 10 quadrature points in the calculations presented here; values for S and J agreed to at least 2 significant figures with those obtained using lower-order quadratures. We performed calculations for DBP in air ($Le \approx 5$) and for water in air ($Le \approx 0.85$). The thermophysical data for DBP was taken from Nguyen *et al.* (1987) and that for water using appropriate fits to the data in Lide (1995).

Figure 1 shows the variation of saturation with scaled radius for DBP at three dimensionless distances along the tube, obtained from the numerical solution. The wall temperature

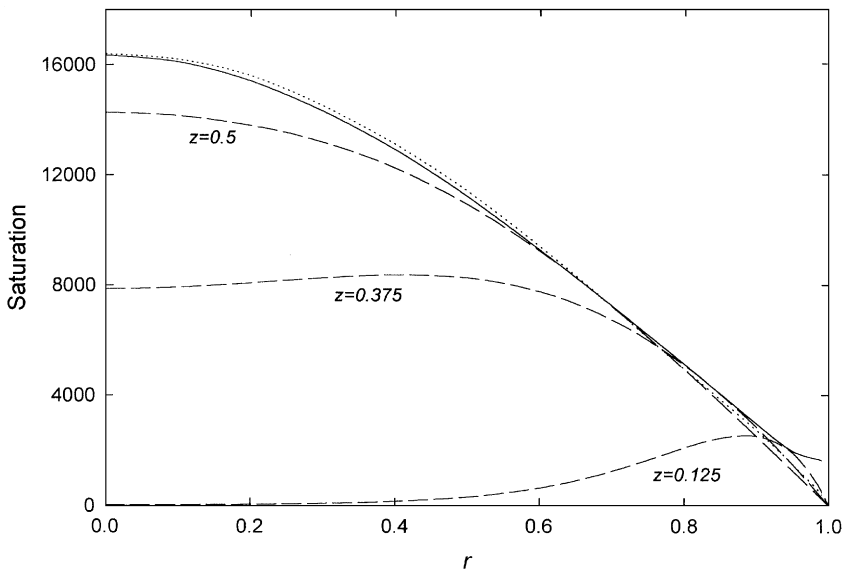


Fig. 1. Variation of saturation with dimensionless radial position at three dimensionless axial positions for DBP in air with $T_w = 273$ K, $\Delta T = 90$ K. Also shown by the solid line is the locus of maximum saturations and by the dotted line, our approximation, equation (9), to it.

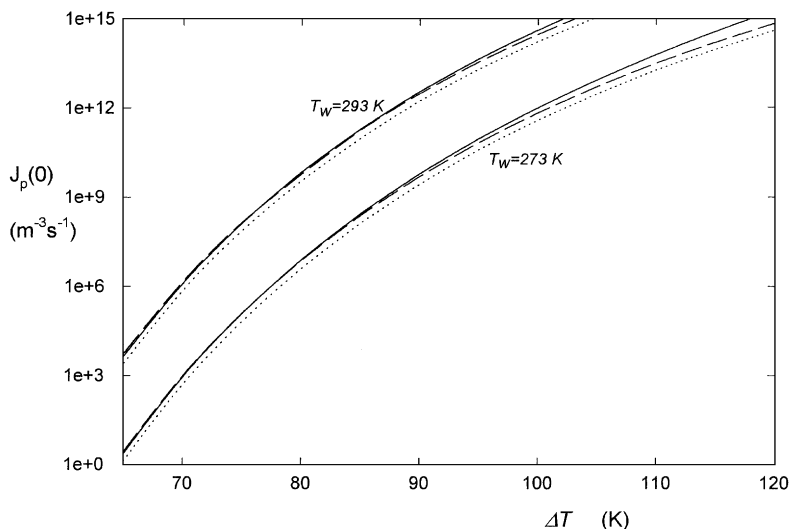


Fig. 2. Variation of peak nucleation rate on the tube axis, $J_p(0)$, with inlet-wall temperature difference, ΔT for DBP in air. The solid lines show values from the numerical solution and the dashed lines show our analytical approximation. Also shown by the dotted lines are the nucleation rates at the position of maximum saturation.

for the case shown is 273 K and the inlet temperature is 363 K. The solid line shows the locus of maximum saturations achieved at any radial distance. Also shown by the dotted line is our approximation to this maximum S curve, from equation (9) (for the approximate calculations we used a simple fit to $\chi_1(r)$; $\chi_1(r) \approx 0.65 r^4 - 1.63 r^2 + 1$ which is accurate to within 3% for $r < 0.9$). As expected, the maximum saturation increases as the tube axis is approached. Note also that near the wall, the maximum saturation achieved does not tend to zero (as predicted by equation (9)), but instead levels off at a value close to that predicted by equation (11) (≈ 1600). Figure 2 shows the maximum nucleation rate on the tube axis ($r = 0$), as a function of inlet-wall temperature difference, and also the nucleation rate at the position of maximum saturation. The latter is between a half and a quarter of the former and the peak saturation occurs a dimensionless distance of between 0.1 to 0.3 after the peak nucleation rate (the peak nucleation rates typically occur at a dimensionless distance of between 0.3 and 0.5). Also shown is the peak nucleation rate $J_p(0)$ calculated by the approximate approach, i.e. at $T_p = T_w + \delta T(1 + \varepsilon)$ and $S_p = S_{\max}$ where δT is given by equation (8), ε by equation (17) and S_{\max} by equation (9) with R in this equation having its value at $r = 0$, i.e. $R = a_1$. The simple approximation very accurately reproduces the numerical results, except at the highest nucleation rates where it underestimates the rate. However, we would not expect the assumption of negligible vapour depletion by growth to be valid at very high nucleation rates (see below). Figure 3 shows the total number of particles (scaled by $r_0^4 V_M / \alpha$) emerging from the tube per second, calculated by performing the integrals over r and z numerically, and from the analytical expression, equation (21). Once again, the two approaches agree very well, with differences being less than 30% over the range shown. Also shown in Fig. 3 are values calculated for n -nonane in Helium, using the thermophysical data tabulated by Rudek *et al.* (1996). Agreement between the two approaches is not as impressive in this case, with approximate values exceeding accurate ones by a factor of about 2. Nevertheless it is quite acceptable, given the large uncertainties in nucleation theories.

We can estimate the maximum nucleation rate for our approach to be valid from inequality (28). We find the various terms in this expression vary rather weakly with temperature (the main variation is the increase in equilibrium vapour density with increasing temperature, and this is compensated for to some extent by the decrease in S_{\max} as T increases); writing the inequality $J_p(0) \ll \kappa / r_0^5$, we find that κ is between 0.5 and 5 for the

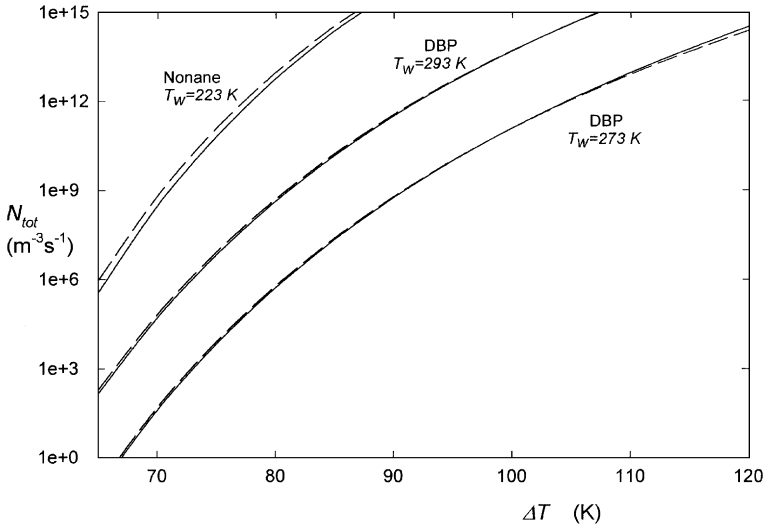


Fig. 3. Total number of particles flowing out of a long tube per second, scaled by $r_0^4 V_M / \alpha$, as a function of inlet-wall temperature difference. The solid lines are from the numerical solution and the dashed lines are from our analytical approximation.

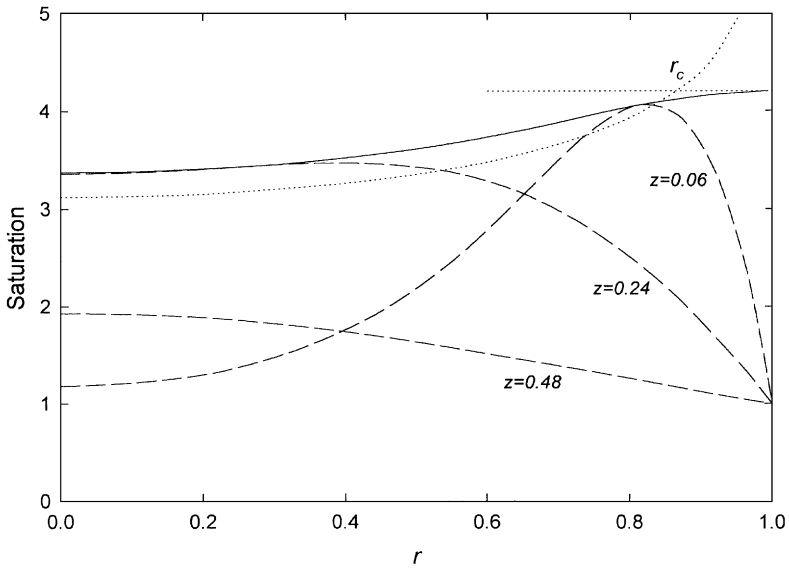


Fig. 4. Variation of saturation with dimensionless radial position at three dimensionless axial positions for water in air with $T_w = 273$ K, $\Delta T = 70$ K. Also shown by the solid line is the locus of maximum saturations. The dotted curve shows S_{max} from equation (9) and the horizontal dotted line shows S_{max} from equation (11). The dimensionless radius at which these two dotted lines intersect is r_c .

conditions we have investigated. Consequently, narrow tubes are required if quenching of nucleation by condensation is to be avoided at moderate nucleation rates (e.g. a nucleation rate of $10^{12} \text{ m}^{-3} \text{ s}^{-1}$ requires a tube radius of less than about 4 mm to avoid this quenching).

Figures 4–6 show some results for water. Figure 4 shows that, as expected, the maximum saturation increases with r , reaching a plateau near the wall. Equation (9) predicts that S_{max} rises to infinity as $r \rightarrow 1$ for $Le < 1$, whereas equation (11) predicts a constant value;

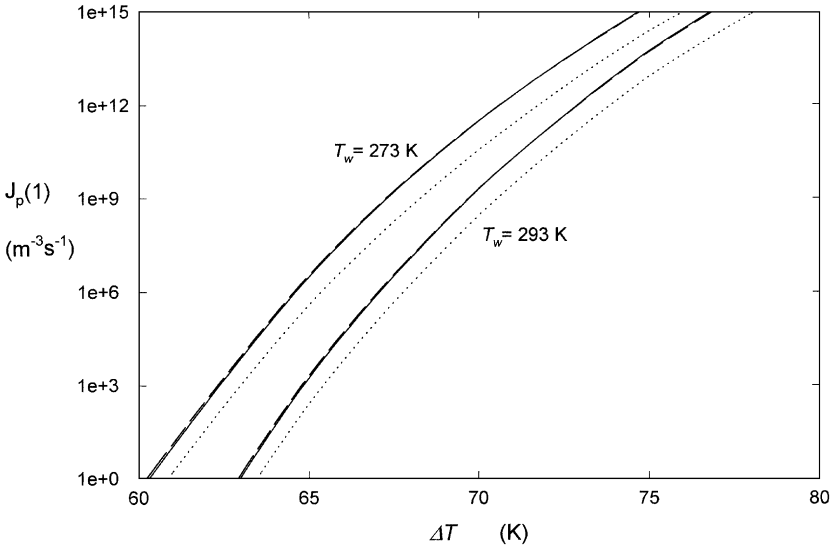


Fig. 5. Variation of peak nucleation rate near the tube wall, $J_p(1)$, with inlet-wall temperature difference, ΔT for water in air. The solid lines show values from the numerical solution evaluated at $r = 0.95$, and the dashed lines show our analytical approximation. Also, shown by the dotted lines are the nucleation rates at the position of maximum saturation.

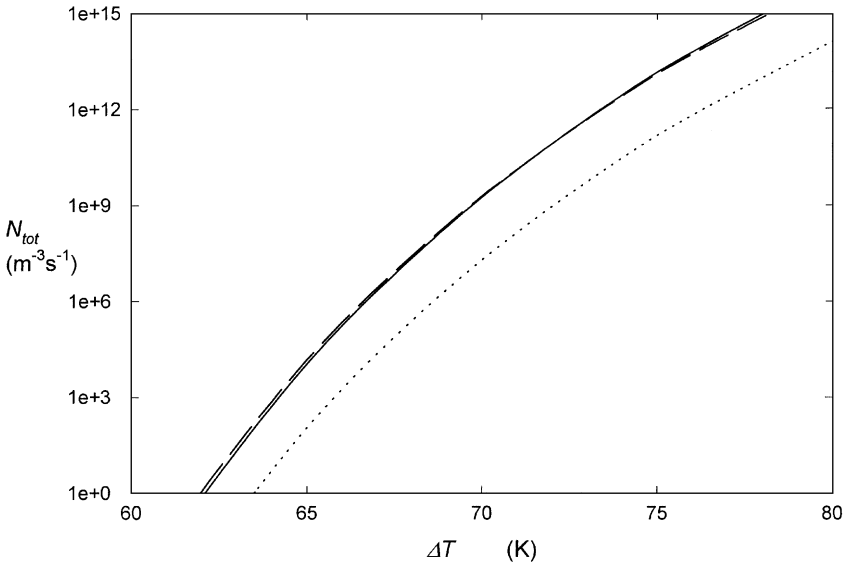


Fig. 6. Total number of water droplets flowing out of a long tube per second, scaled by $r_0^4 V_M / \alpha$, as a function of inlet-wall temperature difference, for $T_w = 273$ K. The solid line is from the numerical solution and the dashed line is from our analytical approximation. The dotted line shows the effect of including the “cross-term” (last term on the left of equation (1)) in the numerical solution.

these two approximations intersect at r_c , given by equation (22). We note that equation (9) significantly underestimates the maximum saturation near the tube axis: we attribute this to the fact that c_w has been set equal to zero in the derivation of this equation. If we set $c_w = 0$ in equations (10) and (11), we obtain a value $S_{\max} \approx 3.9$, significantly less than the value $S_{\max} \approx 4.2$ predicted if these terms are included. Figure 5 shows the maximum nucleation rate near the wall (actually, at $r = 0.95$) and approximate values $J_p(1) = J(S_{\max}, T_p)$

calculated using equation (11) for S_{\max} and equations (10) and (15) to find $T_p = T_w + \delta T_1(1 + \varepsilon)$. Agreement between the numerical and approximate values is very good. Once again, if the terms in equations (10) and (11) involving c_w were ignored, agreement would be much poorer, with approximate predictions underestimating the nucleation rate by a factor of 100 or more. It is interesting to observe in Fig. 5 that, for fixed ΔT , $J_p(1)$ decreases as T_w is increased whereas for DBP, Fig. 2 shows that $J_p(0)$ increases with increasing T_w . Also shown in Fig. 5 is the nucleation rate at the position of maximum saturation, which is seen to be significantly less than the maximum rate. Figure 6 shows values of N_{tot} (scaled by $r_0^4 V_M/\alpha$) for water with $T_w = 273$ K, calculated numerically and from the approximate equation (23). It is notable that the two approaches agree very well, despite the crudity of the approximations involved in the estimate, equation (23). However, also shown in Fig. 6 is the effect of including the “cross term” (last term on the left in equation (1)) in our numerical treatment. As found previously (Barrett and Clement, 1986) this term significantly reduces the saturations, and hence nucleation rates, achieved for water (for low vapour pressure organic vapours, its effect is negligible). Clearly, an accurate estimate of the actual number of water droplets nucleated can only be obtained by taking this term into account.

In principle, we can derive a condition from equation (27) for our approximation to be valid for water, analogous to equation (28) for DBP. However, we have to choose a radius at which the inequality is applied and the right-hand side of equation (27) diverges as $r \rightarrow 1$ (due to the vanishing of σ_z , equation (18), in this limit). Furthermore, particle removal by thermophoresis and diffusiophoresis is likely to be significant near the tube wall due to the large temperature and concentration gradients there. For these reasons, we do not pursue a more detailed analysis of the quenching condition for substances with $Le < 1$.

We now consider the application of our approach to making general predictions in other cases. First we consider the experiments of Hämeri and Kulmala (1996), which have been the subject of a recent very detailed modelling study by Wilck *et al.* (1998). Figure 7 shows a comparison between the experimental results (taken from Fig. 1 of Wilck *et al.*, 1998) and various calculations for the number concentration at the tube outlet, given by N_{tot} divided

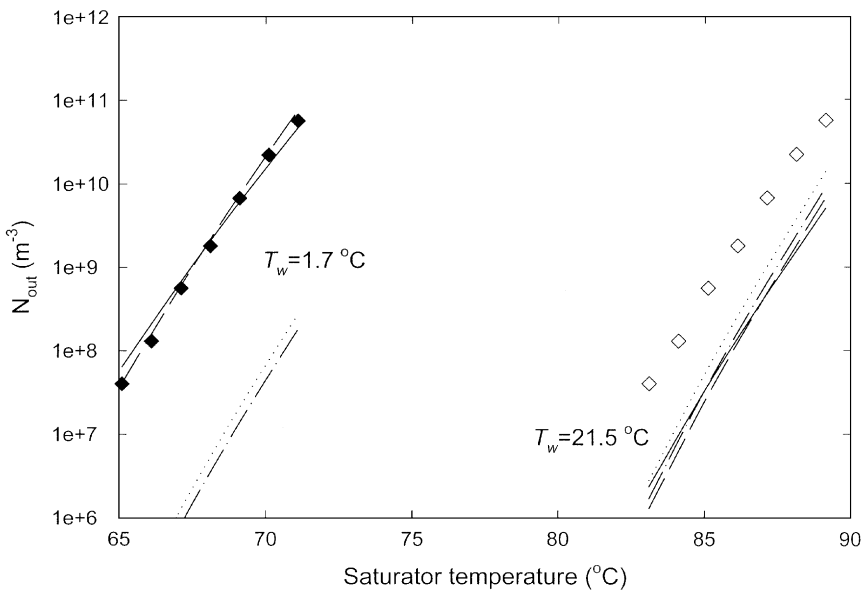


Fig. 7. Variation of particle number concentrations, N_{out} , with saturator (i.e. inlet) temperature for two wall temperatures. The symbols show the experimental measurements taken from Fig. 1 of Wilck *et al.* and the solid and dashed lines show the numerical and approximate analytical predictions, respectively, using their thermophysical data. The dot-dashed and dotted lines show the numerical and analytical predictions using the data used by Nguyen *et al.* For these calculations, the nucleation rate was given by the classical expression (without the $1/S$ factor), enhanced by a factor 10^4 .

by the volumetric flow rate, i.e. $N_{\text{out}} = 2N_{\text{tot}}/\{\pi V_M r_0^2\}$. Note that in this figure only, we have used classical theory (without the $1/S$ factor) enhanced by a factor 10^4 (i.e. equation (3) with $K = 10^4 \sqrt{2\gamma/(\pi m_1)} v_1 (c\rho/m_1)^2$), as used by Wilck *et al.* The solid lines show our numerical calculations using these authors' data and so can be compared with the dotted lines in their Fig. 1. Our values are slightly higher than their ones (by up to about 20%, the difference increasing with saturator temperature): we attribute this to variations of thermal properties and density (and hence velocity profile) with temperature which they model but we do not. The dashed lines show the results of our approximate treatment, with B given by the gradient of the best-fit straight line when $\ln p_{\text{ve}}$ is plotted against $1/T$ over the temperature range of interest. This gives $B = 12,368$ K for the temperature range 275–345 and $B = 11,553$ K for the range 295–385 K. The dashed lines have different slopes from the solid ones, due to the use of constant values of B ; however, agreement between the two approaches is still good. Also, shown are numerical values (dot-dashed lines) and approximate values (dotted lines) using the thermophysical data of Nguyen *et al.* (1987), with $B = 11,497$ K. This lower value of B leads to much lower number concentrations at the lower wall temperature. Since the saturation varies between about 400 and 2000 for the conditions shown, it is clear that including the $1/S$ factor would make agreement between theory and experiment even worse. However, from a theoretical point of view, it is more satisfactory to include this factor (see Oxtoby, 1992).

Other aspects of the numerical results of Wilck *et al.* (1998) can also be explained by our treatment. For example, equation (8) predicts that the temperature difference between the position of peak nucleation and the wall is independent of the inlet temperature, in line with Fig. 5 of Wilck *et al.* (1998) (we attribute the rise in temperature at the highest nucleation rates to vapour depletion effects). Equation (8) gives $\delta T \approx 1.8$ K, which is somewhat smaller than the value of about 2.7 K found by Wilck *et al.* (1998). However, including the ε correction gives better agreement; $\delta T(1 + \varepsilon) \approx 2.4$ K. We can also understand the sensitivities to material properties observed by Wilck *et al.* (1998). Figure 7 of Wilck *et al.* shows that using a smaller value of vapour–gas diffusivity (i.e. a larger value for Le) gave higher particle production rates, whereas using a different vapour pressure equation, corresponding to a smaller value of B , resulted in smaller predicted nucleation. This agrees with the predictions of equation (9): see our comments after that equation. Wilck *et al.* found that quenching becomes important for nucleation rates somewhere between 10^{11} and $10^{12} \text{ m}^{-3} \text{ s}^{-1}$, which is consistent with inequality (28), the right-hand side of which is about $5 \times 10^{12} \text{ m}^{-3} \text{ s}^{-1}$ for this (6 mm) diameter tube.

Finally, we examine the use of our approach to make predictions about the conditions for nucleation to occur in laminar tube flow. Instead of using classical theory (which requires the liquid surface tension and density as functions of temperature), we use a correlation proposed by Hale (1988)

$$\ln S \approx 0.53\Omega^{3/2} \left[1 + \frac{\ln(10^{-6}J)}{144} \right] \left(\frac{T_c}{T} - 1 \right)^{3/2}, \quad (29)$$

which involves two temperature-independent parameters; T_c , the critical temperature of the vapour and Ω , a dimensionless parameter that can be identified as the effective excess surface entropy (in units of the Boltzmann constant) per molecule in the cluster. Equation (29) gives the saturation S needed to achieve a nucleation rate J at temperature T . Hale showed that experimental data for nonane, octane and *n*-butylbenzene was well represented by this equation with $\Omega = 2.35$. Other substances are better represented with lower values of Ω (e.g. for water $\Omega \approx 1.5$).

For given values of B/T_c and Le , we use equation (8) to determine $T = T_w + \delta T$ and then equation (29) to find the value of $S = S_{\text{max}}$ required at this temperature to achieve a specified nucleation rate. Finally, we determine (from equation (9), by iteration) the inlet–wall temperature difference $\Delta T/T_c$ needed to give this maximum saturation on the tube axis (we restrict our attention to substances with $Le > 1$). Figure 8 shows some results

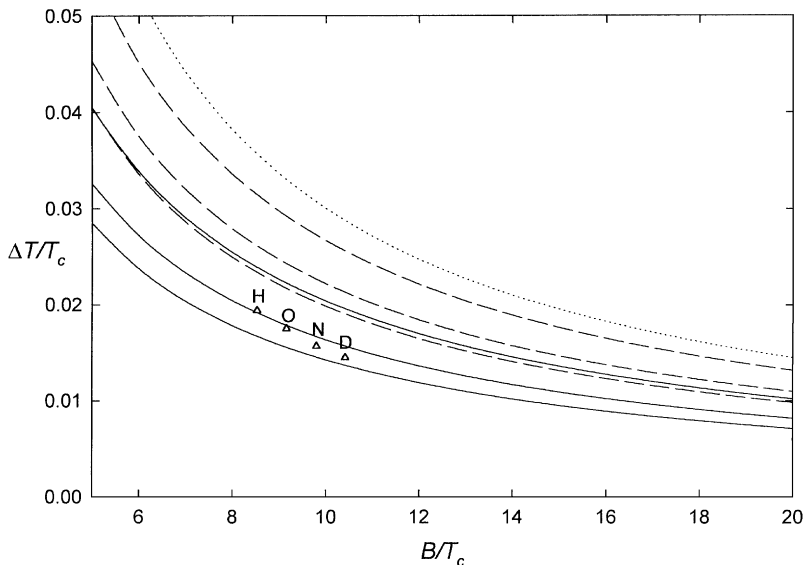


Fig. 8. The solid lines represent the minimum value of $\Delta T/T_c$ for a peak nucleation rate, $J_p(0) = 10^6 \text{ m}^{-3} \text{ s}^{-1}$ as a function of the parameter B/T_c in the equilibrium vapour concentration equation. The dashed lines are for $J_p(0) = 10^{18} \text{ m}^{-3} \text{ s}^{-1}$. In both cases, $T_w = 0.5T_c$ and values are for $Le = 5$ (upper line), $Le = 7.5$ (middle line) and $Le = 10$ (lower line). The dotted line shows the effect of reducing T_w to $0.4T_c$ (for $Le = 5$, and $J_p(0) = 10^{18} \text{ m}^{-3} \text{ s}^{-1}$). The triangles show the values of $\Delta T/T_c$ needed to achieve a peak nucleation rate of $10^6 \text{ m}^{-3} \text{ s}^{-1}$ using the experimental values of Le and B/T_c for heptane (H), octane (O), nonane (N), and decane (D), assuming $T_w = 0.5 T_c$.

from this procedure, assuming $\Omega = 2.35$. For a given value of Le , the lines represent the minimum value of $\Delta T/T_c$ needed to achieve the specified nucleation rate, J , as a function of B/T_c . The four triangles refer to heptane (H), octane (O), nonane (N) and decane (D) and show the values of $\Delta T/T_c$ needed to achieve a nucleation rate of $10^6 \text{ m}^{-3} \text{ s}^{-1}$ for the values of Le and B/T_c applicable to these substances (data for these n -alkanes were taken from Rudek *et al.*, 1996). Figure 8 can be used to predict the experimental conditions needed to achieve the specified nucleation rates for any substance (for which B , Le , and T_c are known). Since the range of B/T_c and Le shown cover expected values for most organic molecules used in laboratory studies, and since values of ΔT of between $0.01T_c$ and $0.05T_c$ should be readily attainable, it also supports the claim (Vohra and Heist, 1996) that the laminar flow diffusion chamber is a useful device for investigating homogeneous nucleation for a variety of substances and nucleation rates. However, the higher nucleation rate, $10^{18} \text{ m}^{-3} \text{ s}^{-1}$, is unlikely to be achieved in practice due to quenching by condensation on nucleated droplets (i.e. inequality (28) will be violated).

4. CONCLUSIONS

We have presented an approximate method of determining the magnitude and location of the nucleation “pulse” that may occur during the laminar flow of hot vapour–gas along a cooled tube. The key parameters are the Lewis number, Le , and the parameter B in the vapour concentration (or vapour pressure) expression. According to the Clausius–Clapeyron equation, $B = m_1 L/k_B$, i.e. the latent heat per molecule in units of Boltzmann’s constant. More generally, B can be defined as the gradient of the best-fit straight line when $\ln p_{ve}$ is plotted against $-1/T$. For $Le > 1$, the maximum saturation occurs on the tube axis but for $Le < 1$, it occurs near the tube wall (and also very near the tube entrance). The magnitude of B influences the magnitude of the maximum saturation achieved (S_{\max} increases with B). Whether significant nucleation is predicted to occur at this saturation depends on the nucleation theory used. No theory is entirely satisfactory for all substances

and temperatures (Oxtoby, 1992); in this paper we have performed calculations using classical theory and also using the correlation, equation (29), proposed by Hale (1988). Using a different nucleation theory will lead to different values of σ_r and σ_z as well as changing J_p ; however we expect the changes in the σ 's to be rather modest (especially since classical theory gives a good representation of the saturation dependence of the nucleation rate) so the classical theory values can still be used. Thus we expect our approximation for N_{tot} , equation (21), to be valid even for nucleation rates that are not of the general form given by equation (3) (note that equation (29) is not of this form). The advantage of Hale's correlation is that it involves only two temperature-independent parameters. However, it should be mentioned that equation (29) is not supported by all experimental data. Kane and El-Shall (1996) found for three glycols that, although plots of $\ln S$ vs $(T_c/T - 1)^{3/2}$ were almost linear, the lines did not pass through the origin and their gradients predicted smaller values (about 1) for Ω . Furthermore, when we plotted the experimental data for DBP from Hämeri and Kulmala (1996) in this way, we found little evidence of a linear relation and the best fit straight lines yielded values of Ω greater than 3, significantly larger than the range 1.5–2.35 proposed by Hale.

Our approximate approach yields good agreement with our accurate calculations, although it should be noted that there are several approximations common to both our analytical and numerical results. The flow is assumed to be laminar (Reynolds number, Re , less than about 2000) and fully developed (requiring a length beyond the tube entrance of the order of $0.07r_0 Re$). Moreover, we have ignored the variation of transport properties and gas density with temperature. We have not carried out a detailed analysis of the errors involved in these approximations, although calculations using properties evaluated at different temperatures indicate that they are small (a few tens of percent in N_{tot}) for the conditions considered here. The reasonable agreement between our numerical results in Fig. 7 and those of Wilck *et al.* (1998), whose modelling included temperature variations and non-parabolic velocity profiles, supports this estimate. We have also ignored diffusion in the axial direction; however the estimates of Vohra and Heist (1996) indicate that this is valid for flow rates typical of laminar diffusion chambers. Other effects not included here, such as thermal diffusion, the Dufour effect and non-ideal gas effects have been found to be significant in interpreting thermal diffusion chamber experiments (Fisk and Katz, 1996) and so may also need to be considered in the interpretation of laminar flow diffusion chamber experiments. It may be possible to incorporate these effects (approximately) in our approach, but we have not investigated this.

To obtain analytical formulae, we have made several additional approximations, the key one being that quenching of nucleation due to vapour consumption by growing droplets can be neglected. A condition has been given for this to be valid (equation (27)), which shows that small diameter tubes are needed if quenching is to be avoided at significant nucleation rates. We have also assumed that the axial displacement at the position of maximum nucleation, z_p , is sufficiently large that simplified forms of the analytical temperature and concentration profiles can be used. This approximation is justified for the results presented here, but should be checked in other circumstances. Finally, for $Le > 1$, we have assumed that the vapour concentration at the wall is negligible. This is reasonable for DBP, with its large value of B , but may not be valid for other vapours—we suspect that the poorer agreement between approximate and numerical results for nonane (see Fig. 3) is due to this approximation.

Our approximate treatment yields reasonable agreement with the accurate calculations of Wilck *et al.* (1998) at the two wall temperatures considered (see Fig. 7). Although we have not performed comparisons at other wall temperatures, we would expect agreement to be similarly good (provided appropriate values of B are used). Our results support the conclusion of these and other authors that a large temperature-dependent correction factor is needed to obtain agreement between theoretical and experimental nucleation rates for DBP. We should add, however, that we would not in general recommend using our approach for detailed comparison between theory and laboratory experiment, due to the approximations discussed above. As noted in the introduction, our principle aim is to make

general predictions about whether nucleation will occur for vapours with poorly known thermal properties, and to identify those properties of greatest importance for predicting nucleation behaviour.

One other aspect of our approach for $Le > 1$ is worth mentioning. We have assumed that the tube is long enough to include the nucleation peak on the tube axis. The saturation peak occurs at a dimensional distance $z'_0 = r_0^2 V_M \ln(\Delta T a_1 / \delta T) / (\alpha \beta_1^2)$ which, for V_M not too large (to ensure laminar flow) is likely to be of the order of centimeters for tube radii of a few millimetres, but may be several metres for tube radii of a few centimetres. The nucleation peak occurs before the saturation peak, but will be at a comparable distance. It is therefore possible that nucleation will occur first near the wall (if equations (10) and (11) predict suitable conditions) but that the tube is too short for it to occur near the axis.

For water, our approximate approach gives accurate estimates of the saturation and nucleation rate near the wall, although there are several aspects of our modelling of water nucleation that should be improved. The assumption that the vapour concentration c is small (implicit in the approximation $S \approx c/c_e(T)$) is not valid for water at the moderate to high temperatures we considered, and we have shown that the “cross-term” in equation (1), which is not currently included in our approximate treatment, has a significant effect on predicted nucleation rates. Furthermore, our experience with modelling water nucleation in other circumstances (Barrett and Clement, 1991; Barrett, 1999) leads us to suspect that our basic assumption that the effects of condensation can be ignored is rarely valid for water. Finally, as we have noted, thermophoresis and diffusiophoresis are expected to have a significant effect on the behaviour of aerosol nucleated near the wall.

Although we have only considered laminar tube flow in this paper, our approximation method is applicable to many other two-dimensional situations where nucleation may occur. The basic requirement is that the temperature and vapour concentration at position (r, z) can be approximated by $\{T_w + \Delta TR(r)Z(z)\}$ and $\Delta cR(r)F(Z(z))$, respectively, with known forms of R , Z , and F . Thus, the approach could be applied to turbulent boundary layers near surfaces and to axisymmetric and planar jets, using standard correlations for the temperature and concentration in these situations. It should also be possible to develop the approach to deal with time dependent and higher-dimensional problems. In all cases, conditions on the nucleation rate, analogous to inequality (27), can be derived for the validity of the basic assumption that vapour depletion by condensation is negligible. For cases where this condition is violated, a general approach has been described recently (Barrett, 2000). We are currently investigating the application of this approach to laminar tube flow.

REFERENCES

- Baldwin, T. J. and Barrett, J. C. (1998) *J. Aerosol Sci.* **29**, S83.
 Barrett, J. C. (2000) *J. Aerosol Sci.* **31** (in press).
 Barrett, J. C. and Clement, C. F. (1986) *J. Aerosol Sci.* **17**, 129.
 Barrett, J. C. and Clement, C. F. (1991) *J. Aerosol Sci.* **22**, 327.
 Barrett, J. C. and Fissan, H. (1989) *J. Colloid Interface Sci.* **130**, 498.
 Clement, C. F. (1985) *Proc. Roy. Soc. A* **398**, 307.
 Finlayson, B. (1972) *The Method of Weighted Residuals and Variational Principles*. Academic Press, New York.
 Fisk, J. A. and Katz, J. L. (1996) *J. Chem. Phys.* **104**, 8649.
 Hale, B. N. (1988) In *Lecture Notes in Physics* (Edited by Wagner P. E. and Vali, G.), Vol. 309, p. 323. Springer, New York.
 Hämeri, K. and Kulmala, M. (1996) *J. Chem. Phys.* **105**, 7696.
 Hämeri, K., Kulmala, M., Krissinel, E. and Kodenov, G. (1996) *J. Chem. Phys.* **105**, 7683.
 Ingham, D. B. (1975) *J. Aerosol Sci.* **6**, 125.
 Kane, D. and El-Shall, M. S. (1996) *J. Chem. Phys.* **105**, 7617.
 Larrode, F. E., Housiadas, C. and Drossinos, Y. (1998) *J. Aerosol Sci.* **29**, S91.
 Lévêque, M. A. (1928) *Ann. Mines* **13**, 201.
 Lide, D. R. (1995) *Handbook of Chemistry & Physics*, 76th Edition, CRC Press, Boca Raton.
 Nguyen, H. V., Okuyama, K., Mimura, T., Kousaka, Y., Flagan, R. C. and Seinfeld, J. H. (1987) *J. Colloid Interface Sci.* **119**, 491.
 Nusselt, W. (1910) *Z. Ver. Dt Ing.* **54**, 1154.
 Oxtoby, D. W. (1992) *J. Phys.: Condens. Matter* **4**, 7627.

- Press, W. H., Teukolsky, S. A., Vetterlin, W. T. and Flannery, B. P. (1992) *Numerical Recipes*, 2nd Edition. Cambridge University Press, Cambridge.
- Rudek, M. M., Fisk, J. A., Chakarov, V. M. and Katz, J. L. (1996) *J. Chem. Phys.* **105**, 4707.
- Vohra, V. and Heist, R. H. (1996) *J. Chem. Phys.* **104**, 382.
- Wilck, M., Hämeri, K., Stratmann, F. and Kulmala, K. (1998) *J. Aerosol Sci.* **29**, 899.

APPENDIX

The derivations in this appendix are given in terms of the slightly more general forms: $\theta(r, z) = R(r)Z(z)$ and $\theta(r, z/Le) = R(r)F(Z(z))$. With appropriate choices of the functions R , Z and F , these include our approximate forms near the tube axis ($R(r) = a_1 \chi_1(r)$, $Z(z) = \exp(-\beta_1^2 z)$ and $F(Z) = Z^{1/Le}$) and near the tube wall ($R(r) = 1 - r$, $Z(z) = 3^{1/3}/\Gamma(1/3)z^{1/3}$) and $F(Z) = ZLe^{1/3}$.

(i) *Derivation of equations (14) and (15)*: We have $T = T_w + \Delta T \cdot R(r) \cdot Z(z)$ and (assuming $c_w \ll \delta c$), $c = \Delta c \cdot R(r)F[Z(z)]$, and hence equation (12) can be written as

$$\frac{2f(T)}{(\ln S)^3} \cdot \frac{dZ}{dz} \left[\frac{\ln S f'(T)}{2 f(T)} \cdot \Delta TR(r) - \frac{\partial}{\partial Z} \left(\ln [c_w + \Delta c \cdot R(r)F(Z)] + \frac{B}{[T_w + \Delta TR(r)Z(z)]} \right) \right] = 0, \quad (A1)$$

where we have used equation (9) for $S(r, z)$. We now equate the terms in square brackets to zero, expand to first order in ε , and use the fact that $S = S_{\max}$ and $\partial S/\partial Z = 0$ at $Z = Z(z_0)$ to obtain

$$\begin{aligned} \frac{\ln(S_{\max})}{2} \frac{f'(T_0)}{f(T_0)} \Delta TR(r) + \left(\frac{\ln(S_{\max})}{2} (\Delta TR(r))^2 \frac{d^2}{dT_0^2} \{ \ln(f(T_0)) \} \right. \\ \left. - \left[\frac{d^2}{dZ_0^2} \{ \ln(F(z_0)) \} - \frac{2B(\Delta TR(r))^2}{T_0^3} \right] \right) Z_0 \varepsilon = 0, \end{aligned} \quad (A2)$$

where $Z_0 = Z(z_0)$ and $T_0 = T(z_0, r) = T_w + \delta T$. We now multiply through by Z_0 noting that $\Delta TR(r)Z_0 = \delta T$, and use classical theory to estimate the second derivative of $\ln(f(T_0))$ with respect to T_0 to be $\approx 3/T_0^2$. Then equation (A2) can be written as

$$\left(-Z_0^2 \frac{d^2}{dZ_0^2} \{ \ln(F(Z_0)) \} + \frac{3 \ln(S_{\max})}{2} \left(\frac{\delta T}{T_0} \right)^2 + \frac{2B\delta T^2}{T_0^3} \right) \varepsilon = -\frac{\ln(S_{\max})}{2} \frac{f'(T_0)}{f(T_0)} \delta T. \quad (A3)$$

Now with $F(Z) = Z^{Le^{-1}}$ (near the tube axis) or $F(Z) = Le^{1/3}Z$ (near the wall), the first term in the bracket on the left is of order Le^{-1} (or 1), whereas the second term is of order $(\delta T/T_0)^2$. Also, the third term is of order $\delta T/(Le \cdot T_0)$ near the axis. This follows from equation (8), which can be written, $B\delta TLe = (T_w + \delta T)^2 - \delta T^2$ (near the wall, $B\delta T \approx (T_w + \delta T)^2 - \delta T^2$ and the term is of order $\delta T/T_0$). Assuming $\delta T \ll T_0$, we can ignore the second and third terms. Using the appropriate forms of $F(Z)$ in equation (A3) then gives equations (14) and (15).

(ii) *Derivation of equations (17) and (18)*: To obtain approximation for σ_z we ignore the variation of J with both K and $f(T)$ near the peak to write (from equation (3)),

$$\begin{aligned} \frac{\partial^2 \ln J}{\partial z^2} = \frac{dZ}{dz} \frac{d}{dZ} \left(\frac{dZ}{dz} \frac{d \ln J}{dZ} \right) \approx \left(\frac{dZ}{dz} \right)^2 \left\{ \left(\frac{2f(T)}{(\ln S)^3} \right) \frac{\partial^2 \ln S}{\partial Z^2} - \frac{6f(T)}{(\ln S)^4} \left(\frac{\partial \ln S}{\partial Z} \right)^2 \right\} \\ + \left(\frac{2f(T)}{(\ln S)^3} \right) \frac{\partial \ln S}{\partial Z} \left(\frac{dZ}{dz} \right) \frac{d}{dZ} \left(\frac{dZ}{dz} \right). \end{aligned} \quad (A4)$$

To evaluate σ_z we equate the second derivative of $\ln J$ from equation (16) to the right-hand side of this equation, where we should evaluate the partial derivatives at the nucleation peak, i.e. at $Z(z_p)$. However, to a good enough approximation we can evaluate them at the saturation peak, $Z(z_0)$. Then all the terms involving $\partial \ln S/\partial Z$ vanish. Furthermore, the second derivative, $\partial^2 \ln S/\partial Z^2$ is given by the terms in square brackets in equation (A2), where, as we have just argued, the term involving B can be ignored. Then we find

$$-\frac{1}{\sigma_z^2} = \left(\frac{dZ_0}{dz} \right)^2 \frac{d^2}{dZ_0^2} \{ \ln(F(Z_0)) \} \frac{2f(T)}{(\ln S_{\max})^3}. \quad (A5)$$

Substituting in the appropriate forms for $Z(z)$ and $F(Z)$ and rearranging yields equations (17) and (18).

(iii) *Derivation of equation (20)*: To evaluate σ_r at the tube axis, we need to find $\partial^2 \ln J_p/\partial r^2$ which, ignoring changes in $f(T)$ and the prefactor K , is given by

$$\frac{\partial^2 \ln J_p}{\partial r^2} = \left(\frac{2f(T)}{(\ln S_{\max})^3} \right) \frac{\partial^2 \ln S_{\max}}{\partial r^2} - \frac{6f(T)}{(\ln S_{\max})^4} \left(\frac{\partial \ln S_{\max}}{\partial r} \right)^2. \quad (A6)$$

Note that J_p is the nucleation rate at the peak saturation so it is S_{\max} (equation (9)) that appears on the right-hand side and not S (equation (6)). At $r = 0$, $\partial S_{\max}/\partial r = 0$ so the second term on the right of equation (A6) vanishes. The derivative in the first term at $r = 0$ can be evaluated from equation (9), putting $R = a_1 \chi_1(r)$,

$$\frac{\partial^2 \ln S_{\max}}{\partial r^2} \approx -(1 - \text{Le}^{-1}) \frac{\chi_1'(r)^2}{\chi_1(r)^2} + (1 - \text{Le}^{-1}) \frac{\chi_1''(r)}{\chi_1(r)} = -2\lambda(1 - \text{Le}^{-1}), \quad (\text{A7})$$

where λ is minus the coefficient of r^2 in $\chi_1(r)$, i.e. $\chi_1(r) = 1 - \lambda r^2 + O(r^4)$. Using equation (A7) in equation (A6) and equating the result to $-1/\sigma_r^2$ gives the expression equation (20) for σ_r .